

Multi-Revolution Transfer for Heliocentric Missions with Solar Electric Propulsion

Alessandro A. Quarta*, Giovanni Mengali and Generoso Aliasi

Department of Civil and Industrial Engineering, University of Pisa, I-56122 Pisa, Italy

Abstract

An extension of the classical method by Alfano, for the analysis of optimal circle-to-circle two-dimensional orbit transfer, is presented for a deep space probe equipped with a solar electric primary propulsion system. The problem is formulated as a function of suitable design parameters, which allow the optimal transfer to be conveniently characterized in a parametric way, and an indirect approach is used to find the optimal steering law that minimizes the required propellant mass. The numerical results, obtained by solving a number of optimal control problems, are arranged into contour plots, characterized by different and well-defined behaviors depending on the value of the initial spacecraft propulsive acceleration, the final orbit radius, and the thruster's specific impulse. The paper presents also a semi-analytical mathematical model for preliminary mission analysis purposes, which is shown to give excellent approximations of the (exact) numerical solutions when the number of revolutions of the spacecraft around the Sun is greater than five. An Earth-Mars cargo mission has been thoroughly investigated to validate the proposed approach. In this case, assuming a propulsion system with a specific impulse of 3000 s (comparable to that installed on the Deep Space 1 spacecraft), the results obtained with the semi-analytical model coincide, from an engineering point of view, with the numerical solutions both in terms of total mission time (about 8.3 years) and propellant mass fraction required (about 17.5%). By decreasing the value of the specific impulse, the differences between the results from the semi-analytical model and the numerical simulations tend to increase. However, good results are still possible if the number of revolutions of the spacecraft around the Sun is close to an integer number.

Nomenclature

\mathbf{a}	=	propulsive acceleration, with $a \triangleq \ \mathbf{a}\ $ [mm/s ²]
g	=	standard gravitational acceleration [m/s ²]
\mathcal{H}	=	Hamiltonian function
$\hat{\mathbf{i}}_r$	=	radial unit vector
$\hat{\mathbf{i}}_\theta$	=	circumferential unit vector
I_{sp}	=	specific impulse [s]
m	=	mass [kg]
n	=	number of revolutions
O	=	Sun's center of mass
P	=	thruster input power [W]
r	=	Sun-spacecraft distance [au]
t	=	time [days]
T	=	dimensionless time parameter, see Eq. (32)
u	=	radial component of spacecraft velocity [km/s]
v	=	circumferential component of spacecraft velocity [km/s]
x	=	auxiliary variable
α	=	thrust angle [rad]
ΔV	=	equivalent velocity variation [km/s]
η	=	thruster efficiency

* Corresponding author.

Email addresses: a.quarta@ing.unipi.it (Alessandro A. Quarta), g.mengali@ing.unipi.it (Giovanni Mengali), g.aliasi@dia.unipi.it (Generoso Alias).

Θ = dimensionless angle parameter, see Eq. (34)

θ = polar angle [rad]

λ = adjoint variable

μ_{\odot} = Sun's gravitational parameter [km^3/s^2]

Subscripts

0 = initial, parking orbit

f = final, target orbit

p = propellant

Superscripts

\cdot = time derivative

\star = optimal

\wedge = unit vector

1 Introduction

The analysis of a circle-to-circle orbit transfer for a spacecraft with a low-thrust propulsion system is a classical problem of spaceflight mechanics (Vallado, 2001; Chobotov, 2002). Usually the problem is addressed within an optimal framework (Lawden, 1963; Marec, 1979; Betts, 2010), looking at the transfer trajectory that links the two circular orbits of given characteristics while minimizing (or maximizing) a suitable scalar performance index. The latter may be given

in terms of propellant mass required for the transfer, as in the case of a spacecraft with an electric propulsion system (Williams and Coverstone-Carroll, 1997, 2000), or flight time, as in the case of a solar sail or another advanced propellantless thruster (Sauer, 1976; McInnes, 2000; Mengali et al., 2008). It is also possible that the performance index be chosen equal to a suitable combination of flight time and propellant mass, as in the case of a hybrid propulsion system (Leipold and Götz, 2002; Mengali and Quarta, 2007).

The use of an optimal approach makes the solution of the problem quite complex, insomuch that no analytical solution exists not only for the general problem, but also in the simplified case of coplanar orbits and propulsive thrust with constant modulus. For these reasons many approximate solutions have been proposed, starting from Edelbaum (1961) in the early '60, whose effectiveness has been demonstrated over the years (Kechichian, 1997; Casalino and Colasurdo, 2007; Kluever, 2011) through a direct comparison with (exact) numerical results. Recently, interesting examples of approximate methods for a rapid estimation of near-optimal low-thrust interplanetary transfers for solar electric propulsion systems have been provided by Kluever (2014), who uses a curve-fitting approach from a database of pre-calculated optimal transfers, and Macdonald (2013), who uses orbit averaging techniques to analyze a circle-to-circle mission scenario.

However, neither the power of modern computers nor the availability of sophisticated optimization algorithms (Betts, 1998, 2000) have decreased the practical importance of obtaining approximate solutions of the optimal transfer in this classical mission scenario. Beside the academic usefulness of an analytical model, one practical reason is that the availability of suitable analytical approximations can provide the required initial guesses for trajectory optimization (numerical) algorithms. In general, the number of free parameters to be managed, such as the initial and final orbits radius and the main characteristics of the propulsion system, makes the parametric study of the optimal transfer a demanding task, especially in the preliminary phase of mission design (in fact, a single, accurate, optimal trajectory calculation requires a computational time

of several minutes on a modern desktop computer) . Indeed, in this phase it is necessary to quickly estimate the impact of a number of possible design choices on mission performance, in order to narrow the succeeding and more refined analysis to a limited number of mission scenarios (Rayman and Williams, 2002).

Among the approximate models that have been proposed for the analysis of a circle-to-circle orbit transfer, it is worth noting the so called “Alfano transfer”. This approach, originally developed by Salvatore Alfano in his M.S. Thesis (Alfano, 1982), is very effective as, with a wise adimensionalization of the free parameters, it collects the numerical solutions of the optimization problem into some contour plots (Alfano and Thorne, 1993) that give a first order estimate of both the optimal flight time and the propellant mass required for the orbit transfer. Two possible cases have been discussed in the literature, assuming either coplanar orbits (Alfano and Thorne, 1994), or a three-dimensional mission scenario (Wiesel and Alfano, 1985). In both cases, it has been shown that accurate results can be obtained when the propulsive acceleration modulus is very small, that is, much less than the local gravitational acceleration. This situation is interesting from a practical viewpoint, as it is representative of a spacecraft equipped with a conventional electric propulsion system (Brophy and Noca, 1998; Racca, 2003). Notably, Alfano’s approach can also be used, with a few modifications, to investigate the performance of a solar sail-based spacecraft (Quarta and Mengali, 2012).

For tractability purposes, the classical Alfano transfer introduces some simplifying assumptions (Alfano and Thorne, 1994). In particular, the propulsive thrust modulus is constant and the propulsion system is assumed to be always thrusting along the whole transfer, thus modeling a low-thrust that is supplied for a prolonged time interval to reach the required velocity variation. This situation well approximates the actual behavior of an interplanetary spacecraft with an electric thruster where the input power is constant with time (for example, a nuclear-powered spacecraft). However such an assumption can lose its validity for a solar-powered spacecraft, i.e. when the thruster input power is supplied by solar arrays. In that case the propulsive thrust

modulus varies with the distance from the Sun depending on the solar array characteristics (Sauer and Atkins, 1972; Bourke and Sauer, 1972).

The aim of this paper is to extend the Alfano's original approach by considering an electric propulsion system with a variable thrust modulus. More precisely, the proposed analysis considers a two-dimensional heliocentric transfer and assumes that the input power to the Power Processing Unit (PPU), which is supplied by solar arrays, varies as the inverse square distance from the Sun (Oh, 2007). This is a reasonable approximation of the actual behavior of the power generation system because, for a preliminary mission analysis, the time degradation of solar arrays (Bourke and Sauer, 1972) and the differences in equilibrium temperature associated to the variable distance from the Sun (Sauer, 1978) can both be neglected. According to the Alfano's original approach, the propulsion system is assumed to be working for the whole transfer and the spacecraft mass variation due to the propellant consumption is taken into account. Moreover, the specific impulse and the operation point of the propulsion system are both constant by assumption. In fact, a more accurate model of the thruster's behaviour would require the propulsion system to be described by a finite number of operation points, each one being characterized by a corresponding set of values of thrust, propellant mass flow rate, and PPU input power. In that case the optimal selection of the operation point would imply a substantial complication of the optimization process (Quarta and Mengali, 2011; Quarta et al., 2013) that is beyond the scope of the Alfano transfer. As stated previously, a possible extension of the model, not implemented in this paper, should take into account the actual variation of the input electric power from the solar arrays during the transfer by including suitable empiric functions that model the time degradation of solar arrays and the dependence of solar array performance on the distance from the Sun.

The paper is organized as follows. The next section describes the mathematical model used for studying the optimal transfer problem between two heliocentric circular and coplanar orbits.

In analogy with Alfano and Thorne (1994), an indirect approach (Betts, 1998, 2000) is used to find the optimal steering law that solves the associated Two-Point Boundary Value Problem (TPBVP). In particular, the problem is formulated as a function of suitable design parameters, which allows the optimal transfer to be characterized in a parametric way. The TPBVP is solved numerically in section 3 and the results are arranged into contour plots. These plots are characterized by different and well defined behaviors depending on the value of the number of revolutions of the spacecraft around the Sun. The identification of such a feature is the starting base for the development of a semi-analytical model that is treated in section 4. In the same section some mission examples are discussed and a comparison is made between the results using the numerical simulations and the semi-analytical approximations. Some remarks about the effectiveness of the algorithm conclude the paper.

2 Mathematical Model

Consider an interplanetary spacecraft with a solar electric propulsion system (SEP) and assume that the input power to the PPU is supplied by solar arrays. According to the literature (Vadali et al., 2000; Mengali and Quarta, 2005), the propulsive acceleration vector \mathbf{a} can be written in the form

$$\mathbf{a} = \frac{2\eta P}{m g I_{sp}} \hat{\mathbf{a}} \quad (1)$$

where η is the thruster efficiency, m is the spacecraft mass, P is the thruster input electric power, g is the standard gravitational acceleration, I_{sp} is the specific impulse, and $\hat{\mathbf{a}} \triangleq \mathbf{a}/\|\mathbf{a}\|$ is the propulsive acceleration unit vector. The time derivative of the spacecraft mass is related to the value of P through the equation

$$\dot{m} = -\frac{2\eta P}{g^2 I_{sp}^2} \quad (2)$$

According to Alfano and Thorne (1994), Eqs. (1)-(2) assume that the propulsion system be thrusting along the whole transfer trajectory, i.e. the spacecraft mass always decreases continuously with time. Note that the presence of coasting arcs during the orbit transfer can be simulated by means of an additional switching parameter that allows the propulsive acceleration modulus and the spacecraft mass variation to be set equal to zero. However such a possibility will not be considered in this simplified mission analysis, because the introduction of the switching parameter would imply a further control variable to be found within the optimization process, with a significant increase in the complexity of both the numerical simulations and the semi-analytical approximations.

At the initial time $t_0 \triangleq 0$ the spacecraft covers a circular parking orbit around the Sun, with a radius equal to r_0 . Assuming that the whole power available to the PPU is supplied to the thrusters (thus neglecting the electric power necessary for the payload and for the other vehicle's subsystems) and assuming that such power varies as the inverse square distance r of the spacecraft from the Sun, Eqs. (1)-(2) may be rewritten as

$$\mathbf{a} = a_0 \left(\frac{r_0}{r} \right)^2 \left(\frac{m_0}{m} \right) \hat{\mathbf{a}} \quad (3)$$

$$\dot{m} = -\frac{a_0 m_0}{g I_{sp}} \left(\frac{r_0}{r} \right)^2 \quad (4)$$

where $m_0 \triangleq m(t_0)$ is the initial spacecraft mass, and

$$a_0 \triangleq \frac{2 \eta P_0}{m_0 g I_{sp}} \quad (5)$$

is the modulus of the initial propulsive acceleration, i.e. the modulus of the vector \mathbf{a} at time t_0 , when the Sun-spacecraft distance is r_0 and the thruster input electric power is $P_0 \triangleq P(r_0)$.

2.1 Equations of motion

Consider a heliocentric polar reference frame $\mathcal{T}(O; r, \theta)$ with origin O at the Sun's center of mass and whose (orthogonal) radial and circumferential unit vectors are $\hat{\mathbf{i}}_r$ and $\hat{\mathbf{i}}_\theta$, respectively, see Fig. 1. In this reference frame, the polar angle θ is measured counterclockwise from the Sun-spacecraft line at time t_0 .

Bearing in mind that the propulsive acceleration vector is given by Eq. (3), the spacecraft (scalar) equations of motion may be written as

$$\dot{r} = u \tag{6}$$

$$\dot{\theta} = \frac{v}{r} \tag{7}$$

$$\dot{u} = -\frac{\mu_\odot}{r^2} + \frac{v^2}{r} + a_0 \left(\frac{r_0}{r}\right)^2 \left(\frac{m_0}{m}\right) \sin \alpha \tag{8}$$

$$\dot{v} = -\frac{uv}{r} + a_0 \left(\frac{r_0}{r}\right)^2 \left(\frac{m_0}{m}\right) \cos \alpha \tag{9}$$

where μ_\odot is the Sun's gravitational parameter, u and v are the radial and circumferential component of the spacecraft velocity, and α is the spacecraft thrust angle defined as (see also Fig. 1)

$$\sin \alpha = \hat{\mathbf{a}} \cdot \hat{\mathbf{i}}_r \quad , \quad \cos \alpha = \hat{\mathbf{a}} \cdot \hat{\mathbf{i}}_\theta \tag{10}$$

The equations of motion are completed by a fifth differential equation, given by Eq. (4), which describes the spacecraft mass variation with time.

Note that the problem is mathematically described by means of a single control variable, the thrust angle α , and by two design parameters, a_0 and I_{sp} , which define the performance of the propulsive system. A suitable variation of a_0 and I_{sp} allows the orbit transfer to be studied in a parametric way as is discussed in the following sections.

2.2 Trajectory Optimization

For a given initial circular parking orbit of radius r_0 and a final circular, coplanar, orbit of given radius r_f , the transfer trajectory is found by solving an optimal control problem in which the propellant mass required to complete the transfer $m_p \triangleq m_0 - m_f$ is the scalar performance index to be minimized, where m_f is the final spacecraft mass. Recalling that, by assumption, the propulsion system is always thrusting, the spacecraft mass decreases continuously with time, while the total mission time represents an output of the optimization process. On the other hand, the same conclusion would be incorrect in the presence of coasting arcs, since in that case the minimization of the propellant mass at an unconstrained final time would correspond to an increasing boundlessly flight time.

The optimal control problem can be addressed using an indirect approach (Betts, 1998, 2000) with the Hamiltonian of the problem defined as

$$\mathcal{H} \triangleq \lambda_r \dot{r} + \lambda_\theta \dot{\theta} + \lambda_u \dot{u} + \lambda_v \dot{v} + \lambda_m \dot{m} \quad (11)$$

where λ_i is the adjoint to the variable i . From Pontryagin's maximum principle the optimal control angle $\alpha = \alpha^*$ is chosen such to maximize \mathcal{H} at any time. Therefore, substituting Eqs.(4) and (6)–(9) into Eq. (11), the optimal thrust angle is

$$\sin \alpha^* = \frac{\lambda_u}{\sqrt{\lambda_u^2 + \lambda_v^2}} \quad , \quad \cos \alpha^* = \frac{\lambda_v}{\sqrt{\lambda_u^2 + \lambda_v^2}} \quad (12)$$

The time variation of the five adjoint variables is given by the Euler-Lagrange equations

$$\dot{\lambda}_r = -\frac{\partial \mathcal{H}}{\partial r} = \lambda_u \left(\frac{v^2}{r^2} - \frac{2\mu_\odot}{r^3} \right) - \frac{\lambda_v u v}{r^2} - \frac{2 a_0 r_0^2 \lambda_m m_0}{r^3 g I_{sp}} + \frac{2 a_0 m_0 r_0^2 \sqrt{\lambda_u^2 + \lambda_v^2}}{m r^3} + \frac{\lambda_\theta v}{r^2} \quad (13)$$

$$\dot{\lambda}_\theta = -\frac{\partial \mathcal{H}}{\partial \theta} = 0 \quad (14)$$

$$\dot{\lambda}_u = -\frac{\partial \mathcal{H}}{\partial u} = \frac{v \lambda_v}{r} - \lambda_r \quad (15)$$

$$\dot{\lambda}_v = -\frac{\partial \mathcal{H}}{\partial v} = \frac{u \lambda_v - 2 v \lambda_u}{r} - \frac{\lambda_\theta}{r} \quad (16)$$

$$\dot{\lambda}_m = -\frac{\partial \mathcal{H}}{\partial m} = \frac{a_0 m_0 r_0^2 \sqrt{\lambda_u^2 + \lambda_v^2}}{m^2 r^2} \quad (17)$$

where the optimal thrust angle, given by Eq. (12), has been taken into account.

The whole differential problem is therefore constituted by ten nonlinear differential equations, including the equations of motion (6)–(9), the equation describing the mass variation (4), and the Euler-Lagrange equations (13)–(17). The differential system must be completed by ten boundary conditions, of which five involve the initial time t_0 , that is

$$r(t_0) = r_0 \quad , \quad \theta(t_0) = 0 \quad , \quad u(t_0) = 0 \quad , \quad v(t_0) = \sqrt{\frac{\mu_\odot}{r_0}} \quad , \quad m(t_0) = m_0 \quad (18)$$

and the other five involve the final time t_f , when the spacecraft reaches the final circular orbit, viz.

$$r(t_f) = r_f \quad , \quad u(t_f) = 0 \quad , \quad v(t_f) = \sqrt{\frac{\mu_\odot}{r_f}} \quad , \quad \lambda_m(t_f) = 1 \quad , \quad \lambda_\theta(t_f) = 0 \quad (19)$$

Recall that t_f is not known a priori (in fact, the final time is an output of the optimization process), whereas the last two conditions of Eq. (19) follow from the application of the transversality condition (Bryson and Ho, 1975). The same transversality condition also implies that

$$\mathcal{H}(t_f) = 0 \quad (20)$$

which allows the flight time t_f to be found. Note that combining $\lambda_\theta(t_f) = 0$ from Eq. (19) with Eq. (14), the result is that $\lambda_\theta = 0$ along the whole optimal trajectory.

The TPBVP consists of finding the initial value of the four adjoint variables λ_r , λ_u , λ_v , λ_m and the flight time t_f such that Eq. (20) and the first four of Eqs. (19) are met. Since the Hamiltonian is not an explicit function of the time [see Eq. (11)], it follows that \mathcal{H} is a constant of motion. Accordingly, from Eq. (20) the result is $\mathcal{H} \equiv 0$ and, using Eq. (11), the adjoint $\lambda_m(t_0)$ can be written as a function of $\lambda_u(t_0)$ and $\lambda_v(t_0)$ as

$$\lambda_m(t_0) = \frac{g I_{sp}}{m_0} \sqrt{\lambda_u^2(t_0) + \lambda_v^2(t_0)} \quad (21)$$

Therefore, the number of scalar variables to be found in the TPBVP is lowered to $\lambda_r(t_0)$, $\lambda_u(t_0)$, $\lambda_v(t_0)$, and t_f .

A set of canonical units is now introduced to reduce the numerical sensitivity of the TPBVP, and in all of the numerical simulations the differential equations have been integrated in double precision using a variable order Adams-Bashforth-Moulton solver scheme (Shampine and Gordon, 1975) with absolute and relative errors of 10^{-12} . In particular, following Alfano and Thorne (1994), the canonical units for the distance (DU), the time (TU), and the mass (MU) are

$$\text{DU} \triangleq r_0 \quad , \quad \text{TU} \triangleq \sqrt{\frac{r_0^3}{\mu_\odot}} \quad , \quad \text{MU} \triangleq m_0 \quad (22)$$

With such a choice the Sun's gravitational parameter, the radius of the initial circular orbit, and the initial spacecraft mass are all unitary. Note that the transfer's performance now depend on three independent parameters, i.e. the final radius r_f , the initial propulsive acceleration a_0 and the specific impulse I_{sp} . Finally, the TPBVP associated to the variational problem has been solved through a hybrid numerical technique that combines genetic algorithms (to obtain a first estimate of the four adjoint variables unknown), with gradient-based and direct methods to refine the solution. Such an approach has been successfully used in various engineering

applications (Bos, 1998; Gudla and Ganguli, 2005).

3 Numerical Results and Graphs

As stated in the previous section, the final spacecraft mass can be obtained numerically as a function of three parameters, i.e. r_f , a_0 , and I_{sp} . To obtain a parametric analysis of the transfer problem, the value of the initial radius has been set equal to $r_0 = 1$ au, and the final radius r_f has been varied within the interval $r_f \in [0.5, 10] r_0$. In other terms, the optimization problem simulates the attainment of either an heliocentric inner circular orbit (if $r_f < r_0$) or an outer circular orbit (if $r_f > r_0$), along the ecliptic plane, for a spacecraft that initially covers the Earth's orbit. The selected range of variation for the specific impulse is $I_{sp} \in [2000, 5000]$ s. This interval includes the typical performance of ion thrusters that have been used so far for missions toward the deep space (Brophy and Noca, 1998; Racca, 2003). As far as the initial propulsive acceleration a_0 is concerned, its value depends on the available thrust and on the initial spacecraft mass m_0 . Since the maximum thrust for an electric propulsion system is typically between some tens and a few hundreds millinewtons, and using a reference initial mass of about 1000 kg, the initial propulsive acceleration is between some hundredths and a few tens of millimeters per square seconds. However, a somewhat larger interval of variation was used in the simulations for the sake of completeness, that is, $a_0 \in [0.01, 2]$ mm/s².

For a generic value of the triplet $\{r_f, a_0, I_{sp}\}$, the optimal (that is maximum) value of the spacecraft final mass $m_f^* \triangleq \max [m(t_f)]$ has been found numerically by solving the corresponding optimization problem. According to Alfano and Thorne (1994) and using the ideal rocket equation, the (maximum) final spacecraft mass may be converted into an equivalent velocity variation ΔV as

$$\Delta V \triangleq g I_{sp} \ln \left(\frac{m_0}{m_f^*} \right) \quad (23)$$

The value of ΔV is useful for comparative purposes with similar results obtained with the classical Alfano's method, in which the mission performance are expressed in terms of accumulated velocity (Alfano and Thorne, 1994). The equivalent dimensionless ΔV (i.e. the ratio $\Delta V/v_0$, where $v_0 \triangleq \sqrt{\mu_\odot/r_0} \approx 29.784$ km/s is the initial circular velocity) is shown in Figs. 2–5 as a function of the triplet $\{r_f, a_0, I_{sp}\}$. For the sake of clarity, the simulation results involve only four different values of the specific impulse, i.e. $I_{sp} \in \{2000, 3000, 4000, 5000\}$ s.

The figures also show the number $n \in \mathbb{N}$ of full revolutions around the Sun completed by the spacecraft before reaching the final orbit, viz.

$$n = \left\lfloor \frac{\theta_f^*}{2\pi} \right\rfloor \quad (24)$$

where $\lfloor \square \rfloor$ is the floor function, and θ_f^* is the final polar angle of the optimal transfer trajectory. For a given mission scenario, the value of n is strongly dependent on the initial value of a_0 and on the radius of the final orbit r_f , whereas the dependence of n on the specific impulse and on ΔV turns out to be scarce in the selected range of I_{sp} .

In particular, Figs. 2–5 reveal a recurrent topology, which allows the figures to be ideally subdivided into three zones, according to the value of n . In fact, when the number of the spacecraft revolutions around the Sun is greater than five, the equivalent velocity variation required for the transfer [or the optimal mass ratio m_f^*/m_0 , see Eq. (23)] is nearly independent of a_0 for a given value of I_{sp} . This result is a consequence of the fact that the gravitational force is dominant over the thrust force. On the contrary, when $n \in [1, 5]$, the variation of ΔV with a_0 has an oscillatory behavior, and the local minima are reached when the spacecraft carries out an integer number of revolutions around the Sun during the transfer. This intermediate region corresponds to a transition zone from thrust dominance to gravitational-force dominance. The last case is when there is a thrust dominance, that is, high values of the initial propulsive accelerations. In that case the final orbit is reached within a fraction of single revolution, i.e.

$\theta_f^* < 2\pi$, and the variation of ΔV increases with a_0 for a given value of I_{sp} . This behavior is consistent with the classical results obtained with the approach by Alfano and Thorne (1994), even if the Alfano transfer assumes a mathematical model substantially different from that adopted here, as previously discussed in the introduction.

Note that within the range of variation of both I_{sp} and r_f considered in this paper, the case $n > 5$ corresponds to an initial propulsive acceleration less than 0.1 mm/s^2 , which is a typical value for an interplanetary mission of a spacecraft propelled by a SEP system (Rayman et al., 2006; Oh, 2007). Such a scenario is therefore particularly interesting and will be used in the next section to discuss a semi-analytical model that permits the transfer performance to be estimated.

4 Semi-analytical Approximation

It is now possible to develop a semi-analytical approximate model for the study of the transfer performance when $n > 5$, that is, under the assumption that the required propellant mass (or ΔV) is nearly independent of the value of the initial propulsive acceleration for a given value of I_{sp} . In this case, since a_0 is much less than the local gravitational acceleration, the spacecraft trajectory resembles a spiral. In other terms, as is confirmed by numerical simulations, during the whole transfer the spacecraft velocity is nearly circumferential and its modulus is close to the local circular velocity, i.e. $v \approx \sqrt{\mu_\odot/r}$. Therefore, an useful approximation of the optimal steering law is $\alpha^* = 0$ or $\alpha^* = \pi$ rad, according to whether the final orbit requires an orbit raising or an orbit lowering, viz.

$$\cos \alpha^* \approx \begin{cases} 1 & \text{if } r_f > r_0 \\ -1 & \text{if } r_f < r_0 \end{cases} \quad (25)$$

In fact, for an orbit raising (lowering) problem, a thrust angle $\alpha^* = 0$ allows the propulsive acceleration to be maximized (minimized) along the direction of the orbital velocity. As stated previously, this optimal propulsive acceleration component is nearly circumferential and, as such, is directed along $\hat{\mathbf{i}}_\theta$.

As a consequence of this last approximation, an analytical expression is now derived for the (maximum) final spacecraft mass when $n > 5$. To that end, combine Eqs. (4) and (9) to get the derivative of the specific angular momentum with respect to the spacecraft mass

$$\frac{d(rv)}{dm} = -\frac{g I_{sp} r \cos \alpha}{m} \quad (26)$$

Substituting $v \approx \sqrt{\mu_\odot/r}$ into Eq. (26) and recalling from Eq. (25) that $\cos \alpha = \cos \alpha^*$ is nearly constant, the result is a separable differential equation. The latter may be integrated to give

$$\frac{m_f^*}{m_0} \simeq \exp \left[\frac{\sqrt{\mu_\odot/r_0}}{g I_{sp} \cos \alpha^*} \left(\sqrt{\frac{r_0}{r_f}} - 1 \right) \right] \quad (27)$$

Equation (27) states that when $n > 5$ the ratio m_f^*/m_0 is independent of the initial propulsive acceleration modulus. Also, substituting Eq. (27) into Eq. (23), the equivalent velocity variation is simply the difference between the initial and final circular velocities, that is

$$\Delta V \approx \frac{\sqrt{\mu_\odot/r_0} - \sqrt{\mu_\odot/r_f}}{\cos \alpha^*} \quad (28)$$

with $\cos \alpha^* \neq 0$, which confirms that ΔV , in this mission scenario, corresponds to the accumulated velocity of the classical Alfano transfer. Note that Eq. (28) is consistent with the ΔV of the Edelbaum model (Chobotov, 2002) in a two-dimensional, circle-to-circle, orbit transfer for a spacecraft with a low propulsive acceleration modulus.

From Eq. (27), an approximation of the total transfer time t_f^* may be easily found. In fact,

the spacecraft mass along the optimal trajectory at an arbitrary time $t \in [t_0, t_f^*]$ (when the spacecraft distance from the Sun is r) is given by

$$\frac{m}{m_0} \approx \exp \left[\frac{\sqrt{\mu_\odot/r_0}}{g I_{sp} \cos \alpha^*} \left(\sqrt{\frac{r_0}{r}} - 1 \right) \right] \quad (29)$$

which is formally identical to Eq. (27), and it is obtained by simply changing m_f^* with m and r_f with r . Substituting Eq. (29) into Eq. (4), the resulting separable differential equation is

$$dt \approx \frac{\sqrt{\mu_\odot/r_0}}{2 a_0 \cos \alpha^*} \sqrt{x} \exp \left[\frac{\sqrt{\mu_\odot/r_0}}{g I_{sp} \cos \alpha^*} \left(\frac{1}{\sqrt{x}} - 1 \right) \right] dx \quad (30)$$

where $x \triangleq \sqrt{r/r_0}$ is an auxiliary, dimensionless, variable. The flight time is therefore

$$t_f^* \approx \frac{\sqrt{\mu_\odot/r_0}}{2 a_0 \cos \alpha^*} T \quad (31)$$

where T is a dimensionless parameter defined as

$$T \triangleq \int_1^{(r_f/r_0)} \sqrt{x} \exp \left[\frac{\sqrt{\mu_\odot/r_0}}{g I_{sp} \cos \alpha^*} \left(\frac{1}{\sqrt{x}} - 1 \right) \right] dx \quad (32)$$

The right hand side integral of Eq. (32) can be calculated numerically as a function of r_f and I_{sp} . The isocontour lines of $T = T(r_f, I_{sp})$ are shown in Fig. 6.

In a similar way it is possible to find a semi-analytical expression for θ_f^* , the angle swept along the optimal transfer. To that end substituting the approximation $v \approx \sqrt{\mu_\odot/r}$ into Eq. (7) and recalling Eq. (30) yields

$$\theta_f^* \approx \frac{\mu_\odot/r_0^2}{2 a_0 \cos \alpha^*} \Theta \quad (33)$$

where Θ is a dimensionless parameter defined as

$$\Theta \triangleq \int_1^{(r_f/r_0)} \frac{1}{x} \exp \left[\frac{\sqrt{\mu_\odot/r_0}}{g I_{sp} \cos \alpha^*} \left(\frac{1}{\sqrt{x}} - 1 \right) \right] dx \quad (34)$$

Similar to T , the integral in Eq. (34) may be evaluated numerically and the results are shown in Fig. 7.

To summarize, Eqs. (27), (31) and (33) along with Figs. (6) and (7) represent a set of semi-analytical relationships that are useful for obtaining a first estimate of the mission performance when $n > 5$, that is when the initial propulsive acceleration modulus is sufficiently small and r_f is substantially different from r_0 , for the selected range of the specific impulse. These results are of practical relevance as the very low-thrust mission case is a demanding task from a numerical point of view due to the long flight times that are necessary for a solution to be found. The effectiveness of the obtained approximations is now demonstrated by discussing a typical mission application for an Earth-Mars cargo mission.

4.1 Mission Applications

Consider an Earth-Mars cargo mission, in which a spacecraft of mass $m_0 = 3000$ kg is equipped with an SEP system with a specific impulse $I_{sp} = 3000$ s, capable of generating an initial propulsive acceleration modulus of $a_0 = 0.03$ mm/s². This case resembles the characteristics of NASA's NSTAR ion thruster (that is, the thruster installed on the Deep Space 1 spacecraft), whose maximum thrust level was about 90 mN with a specific impulse on the order of 3100 s (Brophy et al., 2000) .

Assuming that the spacecraft leaves the Earth with zero hyperbolic excess velocity and that the orbits of the two planets are circular and coplanar with radius $r_0 = 1$ au for the Earth and $r_f = 1.524$ au for Mars, from Fig. 3(a) the (optimal) equivalent velocity variation is $\Delta V \approx$

$0.19 v_0 \approx 5.66$ km/s. Recall that the curves shown in Fig. 3(a), are obtained using numerical optimization methods. From Eq. (23) the corresponding final mass ratio is $m_f^*/m_0 \approx 0.825$ and the minimum propellant consumption is about 525 kg. These values are, as expected, in perfect agreement with the results that can be obtained by numerically solving the optimal problem with an indirect approach (Betts, 1998, 2000). In particular, the numerical simulations state that $m_f^*/m_0 = 0.8251$, $\theta_f^* = 37.751$ rad and $t_f^* = 3031$ days (about 8.3 years) .

The optimal transfer trajectory and the variation of the two spacecraft velocity components (expressed in dimensionless form through the local circular velocity $\sqrt{\mu_\odot/r}$) are shown in Fig. 8 as a function of the polar angle θ . From Fig. 8(a) it is clear that the spacecraft velocity modulus is nearly coincident with the local circular velocity, whereas the whole transfer requires about six full revolutions around the Sun as is confirmed by Fig. 3(a). The time history of the thrust angle α is shown in Fig. 9. Note that the value of $|\alpha|$ is very close to zero (i.e., the thrust is nearly circumferential) along the whole transfer trajectory.

Since the number of full revolutions to reach the target is greater than five, it is possible to use the previously discussed semi-analytical model for comparative purposes. Setting $\cos \alpha^* = 1$, see Eq. (25), from Eq. (27) the optimal mass ratio is $m_f^*/m_0 = 0.8251$. Moreover from Eq. (34) (equivalently, from Fig. 7(a)) $\Theta \approx 0.382$ and Eq. (33) yields $\theta_f^* \approx 37.757$ rad. Finally, using either Eq. (32) or Fig. 6, the value of the dimensionless time parameter is $T \approx 0.527$ and, from Eq. (31), the total flight time is $t_f^* \approx 3030$ days. These results are all nearly coincident, being the differences less than 1%, with the outputs of the numerical simulations, and demonstrate the effectiveness of the approximate semi-analytical model when the triplet $\{r_f, a_0, I_{sp}\}$ corresponds to a value of $n > 5$.

It is worth noting that the approximate relationships derived above are actually able to give a reasonable estimate of the mission performance even if $n < 5$. For example, assume that the same Earth-Mars mission with the same propulsion system (i.e. same I_{sp} and same initial

thrust modulus) is now performed with a spacecraft of mass $m_0 = 1000$ kg. In other terms, the initial propulsive acceleration modulus is increased by a factor three when compared to the previous example and is now equal to $a_0 = 0.09$ mm/s². The numerical simulations for this case state that $m_f^*/m_0 = 0.825$, $t_f^* = 1013$ days (2.8 years) , and $\theta_f^* = 12.56$ rad, corresponding to about two full revolutions around the Sun ($n \approx 2$). Note that, as a consequence of the increase of propulsive acceleration, the values of trip time and transfer angle are both reduced by about 1/3. The semi-analytical model gives excellent results, that is $m_f^*/m_0 \approx 0.825$, $t_f^* \approx 1010$ days, and $\theta_f^* \approx 12.58$ rad.

However, if the initial propulsive acceleration modulus is still further increased up to $a_0 = 0.105$ mm/s², the results from the numerical simulations are $m_f^*/m_0 = 0.81$, $t_f^* = 904$ days, and $\theta_f^* = 11.19$ rad, while the semi-analytical model returns $m_f^*/m_0 \approx 0.825$, $t_f^* \approx 866$ days, and $\theta_f^* \approx 10.78$ rad. In this case the differences between numerical and analytical results become significant, on the order of 4%. The reason for such a discrepancy is that according to the semi-analytical model, the optimal final mass is independent of the initial propulsive acceleration modulus a_0 . On the contrary Fig. 3(a) shows that increasing a_0 produces an oscillation of the final m_f . However, the corresponding local minima are still close to the results that can be obtained when a_0 tends to zero. Since the local minima of $m_f = m_f(a_0)$ are reached when the spacecraft makes an integer number of revolutions it can be concluded, when $n < 5$, that the estimate of m_f from the semi-analytical model is reasonable provided the actual number of revolutions is close to an integer number.

5 Conclusions

A thorough analysis has been presented for the heliocentric transfer between circular and coplanar orbits of a spacecraft with a solar electric propulsion system. According to the classical Alfano transfer, the proposed method uses an indirect approach to find the minimum propellant

mass required for the mission. For sufficiently large numbers of spacecraft revolutions around the Sun, the method provides accurate semi-analytical relationships for the equivalent velocity variation, the flight time, the propellant mass and the total polar angle as a function of the main design parameters. For example, using an Earth-Mars cargo mission as a representative test case, the semi-analytical model is able to give approximations of the exact numerical solutions with errors on the order of 0.5% or less. A full set of simulation results is also presented using suitable charts, thus allowing the designer to obtain a rapid and accurate estimate of the impact of a parameter variation on the mission performance. The set of approximate relationships and charts is well suited for a preliminary mission analysis, because the effectiveness of the model has been verified by comparing the numerical data and the approximate formulas for some reference mission applications.

References

- Alfano, S.. Low thrust orbit transfer. Master's thesis, School of Engineering, Air Force Institute of Technology, Wright-Patterson AFB (OH), AFIT/GA/AA/82D-2, 1982.
- Alfano, S., Thorne, J. D.. Constant-thrust orbit-raising transfer charts. Tech. Rep. PL-TR-93-1010, Phillips Laboratory, Space and Missiles Technology Directorate, Kirtland Air Force Base, NM 87117-5776, available online (cited June 28, 2014) <http://www.dtic.mil/dtic/tr/fulltext/u2/a269088.pdf>, 1993.
- Alfano, S., Thorne, J. D., Circle-to-circle constant-thrust orbit raising. *J. Astronaut. Sci.* 42 (1), 35–45, 1994.
- Betts, J. T., Survey of numerical methods for trajectory optimization. *J. Guid. Control Dynam.* 21 (2), 193–207, doi: 10.2514/2.4231, 1998.
- Betts, J. T., Very low-thrust trajectory optimization using a direct SQP method. *J. Comput. Appl. Math.* 120 (1), 27–40, doi: 10.1016/S0377-0427(00)00301-0, 2000.
- Betts, J. T., *Practical Methods for Optimal Control and Estimation Using Nonlinear*

- Programming, 2nd Edition. *Advances in Design and Control*. Society for Industrial & Applied Mathematics, pp. 265–271, ISBN: 0-898-71688-8, 2010.
- Bos, A., Aircraft conceptual design by genetic/gradient-guided optimization. *Eng. Appl. Artif. Intel.* 11 (3), 377–382, doi: 10.1016/S0952-1976(98)00009-8, 1998.
- Bourke, R. D., Sauer, G. G. J., The effect of solar array degradation on electric propulsion spacecraft performance. In: *AIAA 9th Electric Propulsion Conference*. Bethesda, MD, USA, paper AIAA 72-444, April 17–19 1972.
- Brophy, J. R., Kakuda, R. Y., Polk, J. E., Anderson, J. R., Marcucci, M. G., Brinza, D., Henry, M. D., Fujii, K. K., Mantha, K. R., Stocky, J. F., Sovey, J., Patterson, M., Rawlin, V., Hamley, J., Bond, T., Christensen, J., Cardwell, H., Benson, G., Gallagher, J., Matranga, M., Ion propulsion system (NSTAR) DS1 technology validation report. Tech. Rep. JPL 00-10, Jet Propulsion Laboratory, 4800 Oak Grove Ave., Pasadena, CA 91109, October 2000.
- Brophy, J. R., Noca, M., Electric propulsion for solar system exploration. *J. Propul. Power* 14 (5), 700–707, doi: 10.2514/2.5332, 1998.
- Bryson, A. E., Ho, Y. C., *Applied Optimal Control*. Hemisphere Publishing Corporation, New York, NY, Ch. 2, pp. 71–89, ISBN: 0-891-16228-3, 1975.
- Casalino, L., Colasurdo, G., Improved Edelbaum’s approach to optimize low earth/geostationary orbits low-thrust transfers. *J. Guid. Control Dynam.* 30 (5), 1504–1511, doi: 10.2514/1.28694, 2007.
- Chobotov, V. A., *Orbital Mechanics*, 3rd Edition. AIAA Education Series. American Institute of Aeronautics and Astronautics, New York, Ch. 14, ISBN: 1-56347-537-5, 2002.
- Edelbaum, T. N., Propulsion requirements for controllable satellites. *ARSJ-Am. Rocket Soc. J.* 31, 1079–1089, 1961.
- Gudla, P. K., Ganguli, R., An automated hybrid genetic-conjugate gradient algorithm for multimodal optimization problems. *Appl. Math. Comput.* 167 (2), 1457–1474, doi: 10.1016/j.amc.2004.08.026, 2005.
- Kechichian, J. A., Reformulation of Edelbaum’s low-thrust transfer problem using optimal

- control theory. *J. Guid. Control Dynam.* 20 (5), 988–994, doi: 10.2514/2.4145, 1997.
- Kluever, C. A., Using Edelbaum’s method to compute low-thrust transfers with Earth-shadow eclipses. *J. Guid. Control Dynam.* 34 (1), 300–303, doi: 10.2514/1.51024, 2011.
- Kluever, C. A., Efficient Computation of Optimal Interplanetary Trajectories Using Solar Electric Propulsion. *J. Guid. Control Dynam.* doi: 10.2514/1.G000144, in press.
- Lawden, D. F., *Optimal Trajectories for Space Navigation*. Butterworths, London, pp. 54–68, 1963.
- Leipold, M., Götz, M., January 2002. Hybrid photonic/electric propulsion. Tech. Rep. SOL4-TR-KTH-0001, Kayser-Threde GmbH, Munich, Germany, ESA contract No. 15334/01/NL/PA, 2002.
- Macdonald, M., Analytical, circle-to-circle low-thrust transfer trajectories with plane change. In: *AIAA Guidance, Navigation and Control Conference*. Boston, Massachusetts, AIAA paper 2013-5026, August 19–22 2013.
- Marec, J. P., *Optimal Space Trajectories*. Studies in Astronautics. Elsevier, pp. 1–18, 307–318, ISBN: 0-444-41812-1, 1979.
- McInnes, C. R., Payload mass fractions for minimum-time trajectories of flat and compound solar sails. *J. Guid. Control Dynam.* 23 (6), 1076–1078, doi: 10.2514/2.4651, 2000.
- Mengali, G., Quarta, A. A., Fuel-optimal, power-limited rendezvous with variable thruster efficiency. *J. Guid. Control Dynam.* 28 (6), 1194–1199, doi: 10.2514/1.12480, 2005.
- Mengali, G., Quarta, A. A., Trajectory design with hybrid low-thrust propulsion system. *J. Guid. Control Dynam.* 30 (2), 419–426, doi: 10.2514/1.22433, 2007.
- Mengali, G., Quarta, A. A., Janhunen, P., Electric sail performance analysis. *J. Spacecraft Rockets* 45 (1), 122–129, doi: 10.2514/1.31769, 2008.
- Oh, D. Y., Evaluation of solar electric propulsion technologies for discovery-class missions. *J. Spacecraft Rockets* 44 (2), 399–411, doi: 10.2514/1.21613, 2007.
- Quarta, A. A., Mengali, G., Minimum-time space missions with solar electric propulsion. *Aerosp. Sci. Technol.* 15 (5), 381–392, doi: 10.1016/j.ast.2010.09.003, 2011.

- Quarta, A. A., Mengali, G., A semi-analytical method for the analysis of solar sail heliocentric orbit raising. *J. Guid. Control Dynam.* 35 (1), 330–335, doi: 10.2514/1.55101, 2012.
- Quarta, A. A., Izzo, D., Vasile, M., Time-optimal trajectories to circumsolar space using solar electric propulsion. *Adv. Space Res.* 51 (3), 411–422, doi: 10.1016/j.asr.2012.09.012, 2013.
- Racca, G. D., New challenges to trajectory design by the use of electric propulsion and other new means of wandering in the solar system. *Celest. Mech. Dynamical Astronomy* 85 (1), 1–24, doi: 10.1023/A:1021787311087, 2003.
- Rayman, M. D., Fraschetti, T. C., Raymond, C. A., Russell, C. T., Dawn: A mission in development for exploration of main belt asteroids Vesta and Ceres. *Acta Astronaut.* 58 (11), 605–616, doi: 10.1016/j.actaastro.2006.01.014, 2006.
- Rayman, M. D., Williams, S. N., Design of the first interplanetary solar electric propulsion mission. *J. Spacecraft Rockets* 39 (4), 589–595, doi: 10.2514/2.3848, 2002.
- Sauer, Jr, C. G., Optimum solar-sail interplanetary trajectories. In: *AIAA/AAS Astrodynamics Conference*. San Diego, CA, AIAA paper 76-792, August 18–20 1976.
- Sauer, Jr., C. G., Modeling of thruster and solar array characteristics in the JPL low-thrust trajectory analysis. In: *13th International Electric Propulsion Conference*. San Diego, CA, paper AIAA 78-645, April 25–27 1978.
- Sauer, Jr, C. G., Atkins, K. G., Potential advantages of solar electric propulsion for outer planet orbiters. In: *AIAA 9th Electric Propulsion Conference*. Bethesda, MD, AIAA paper 72-423, April 17–19 1972.
- Shampine, L. F., Gordon, M. K., *Computer Solution of Ordinary Differential Equations: The Initial Value Problem*. W. H. Freeman & Co Ltd, San Francisco, Ch. 10, ISBN: 0-716-70461-7, 1975.
- Vadali, S. R., Nah, R. S., Braden, E., Johnson, I. L., Fuel-optimal planar Earth-Mars trajectories using low-thrust exhaust-modulated propulsion. *J. Guid. Control Dynam.* 23 (3), 476–482, doi: 10.2514/2.4553, 2000.
- Vallado, D. A., *Fundamentals of Astrodynamics and Applications*, 2nd Edition. Microcosm

Press/Kluwer Academic Publisher, Ch. 6, pp. 358–374, ISBN: 1-88188-314-0, 2001.

Wiesel, E. E., Alfano, S., Optimal many-revolution orbit transfer. *J. Guid. Control Dynam.* 8 (1), 155–157, doi: 10.2514/3.19952, 1985.

Williams, S. N., Coverstone-Carroll, V., Benefits of solar electric propulsion for the next generation of planetary exploration missions. *J. Astronaut. Sci.* 45 (2), 143–159, 1997.

Williams, S. N., Coverstone-Carroll, V., Mars missions using solar electric propulsion. *J. Spacecraft Rockets* 37 (1), 71–77, doi: 10.2514/2.3528, 2000.

List of Figures

1	Reference frame and spacecraft thrust angle.	27
2	Transfer performance as a function of a_0 and r_f with $I_{sp} = 2000$ s.	28
3	Transfer performance as a function of a_0 and r_f with $I_{sp} = 3000$ s.	29
4	Transfer performance as a function of a_0 and r_f with $I_{sp} = 4000$ s.	30
5	Transfer performance as a function of a_0 and r_f with $I_{sp} = 5000$ s.	31
6	Dimensionless time parameter T as a function of r_f and I_{sp} , see Eq. (32).	32
7	Dimensionless angle parameter Θ as a function of r_f and I_{sp} , see Eq. (34).	33
8	Earth-Mars optimal circle-to-circle transfer when $a_0 = 0.03$ mm/s ² , $I_{sp} = 3000$ s.	34
9	Thrust angle time history (Earth-Mars transfer, $a_0 = 0.03$ mm/s ² , $I_{sp} = 3000$ s).	35

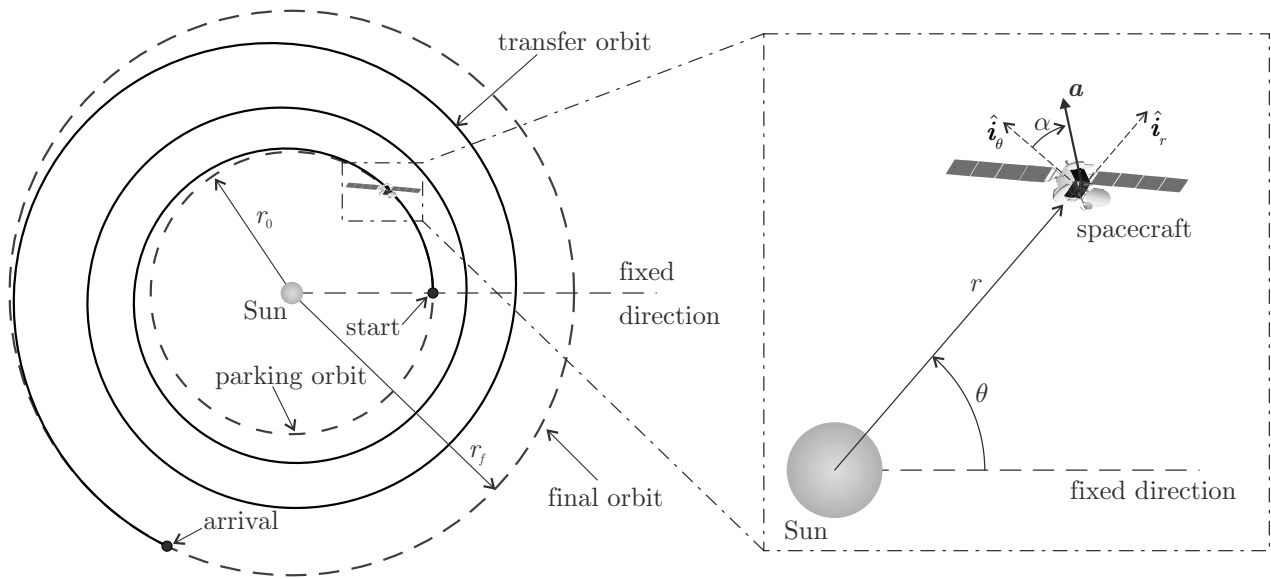
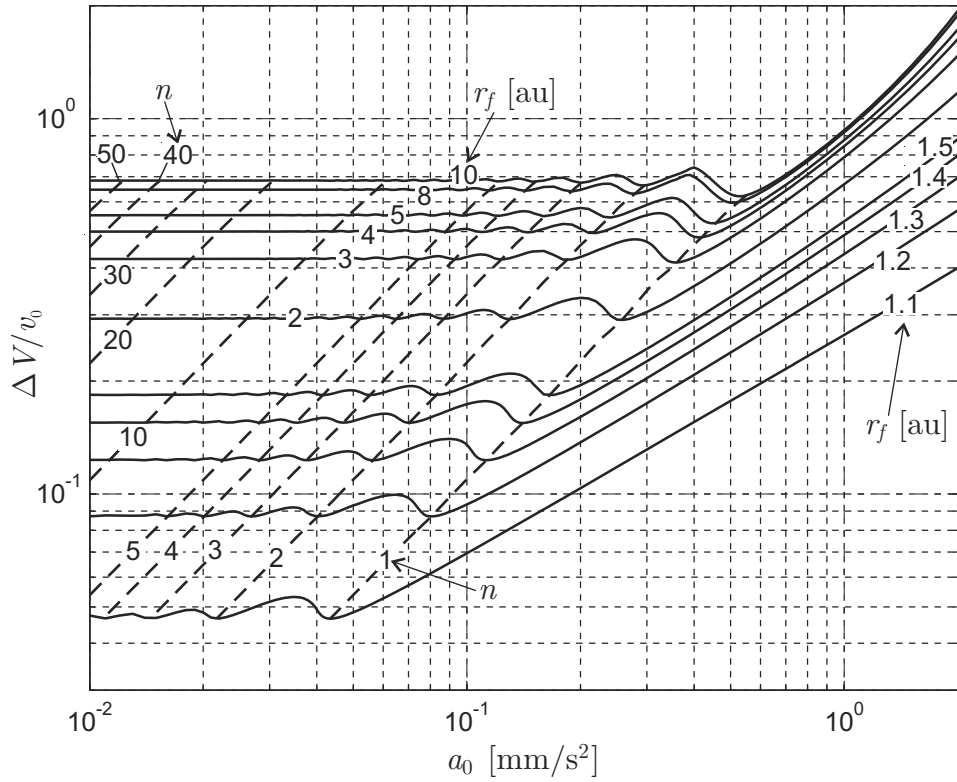
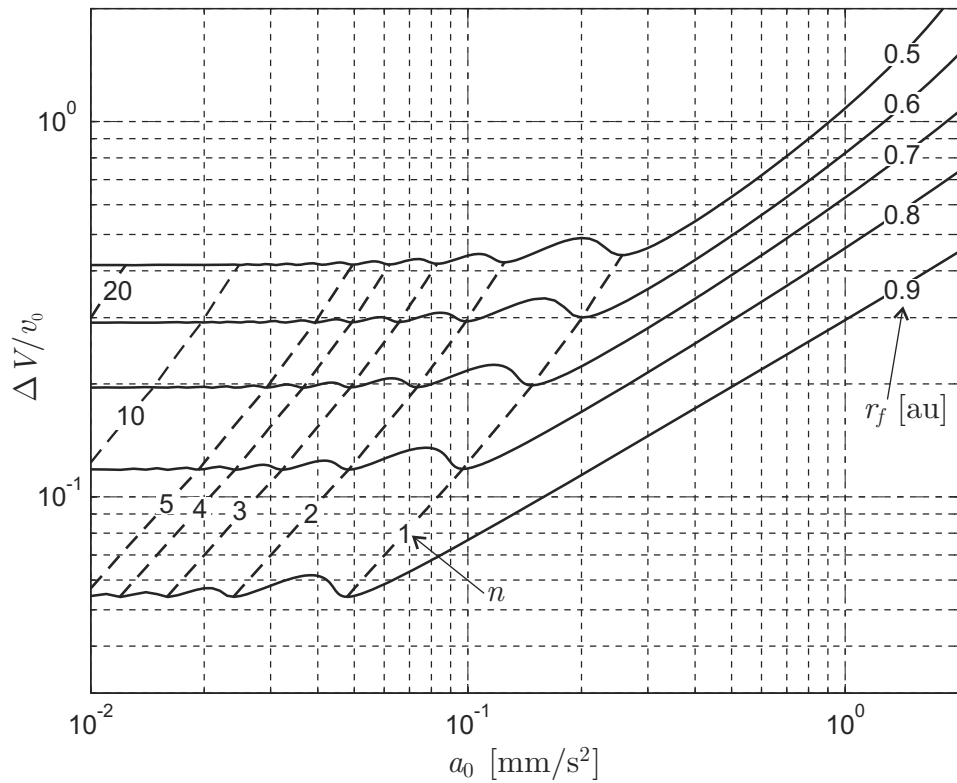


Figure 1. Reference frame and spacecraft thrust angle.

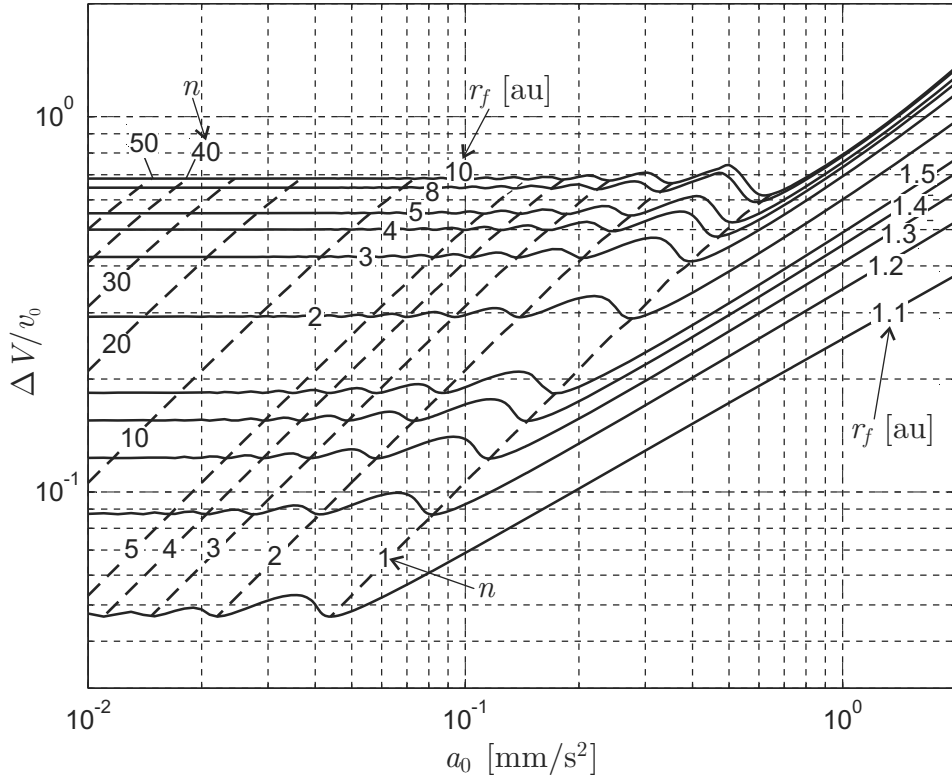


(a) Outer transfer ($r_f > r_0$).

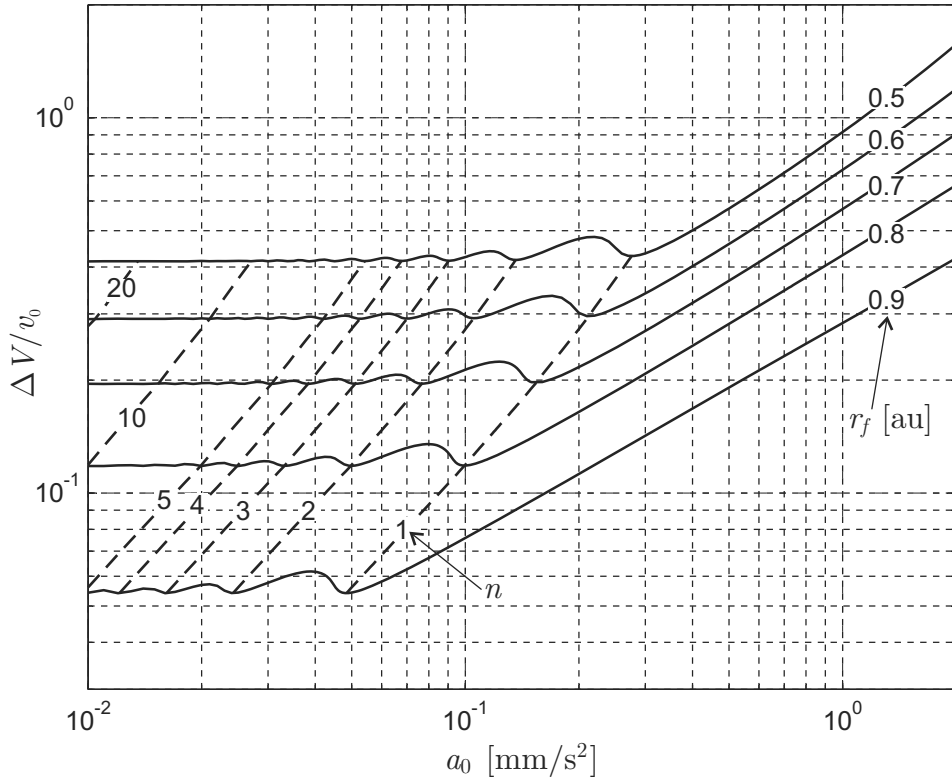


(b) Inner transfer ($r_f < r_0$).

Figure 2. Transfer performance as a function of a_0 and r_f with $I_{sp} = 2000$ s.

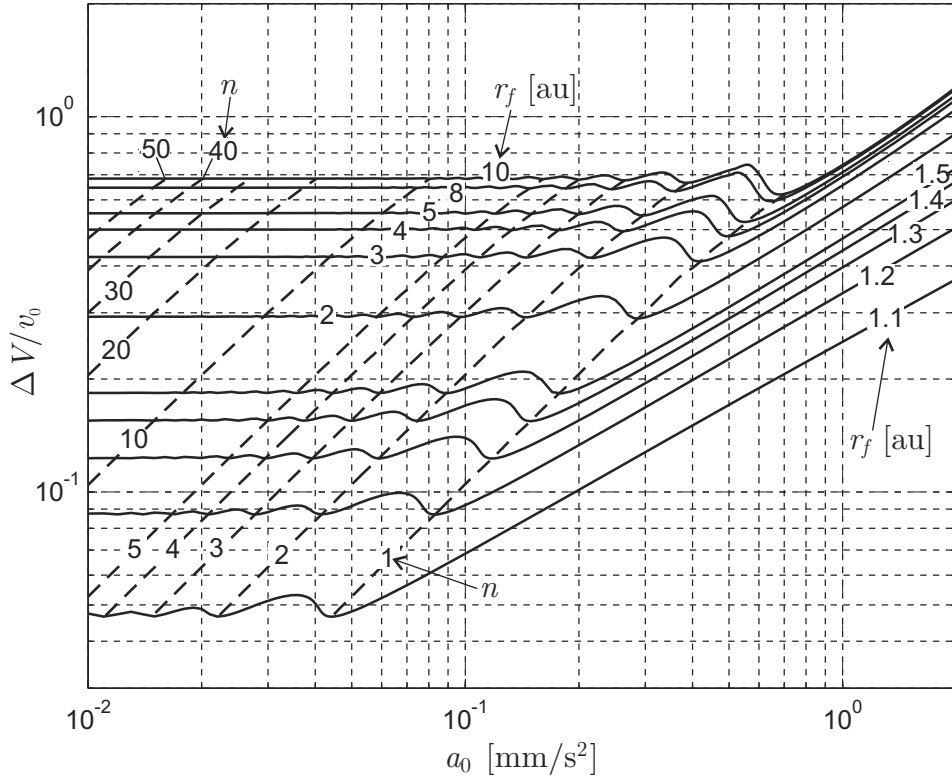


(a) Outer transfer ($r_f > r_0$).

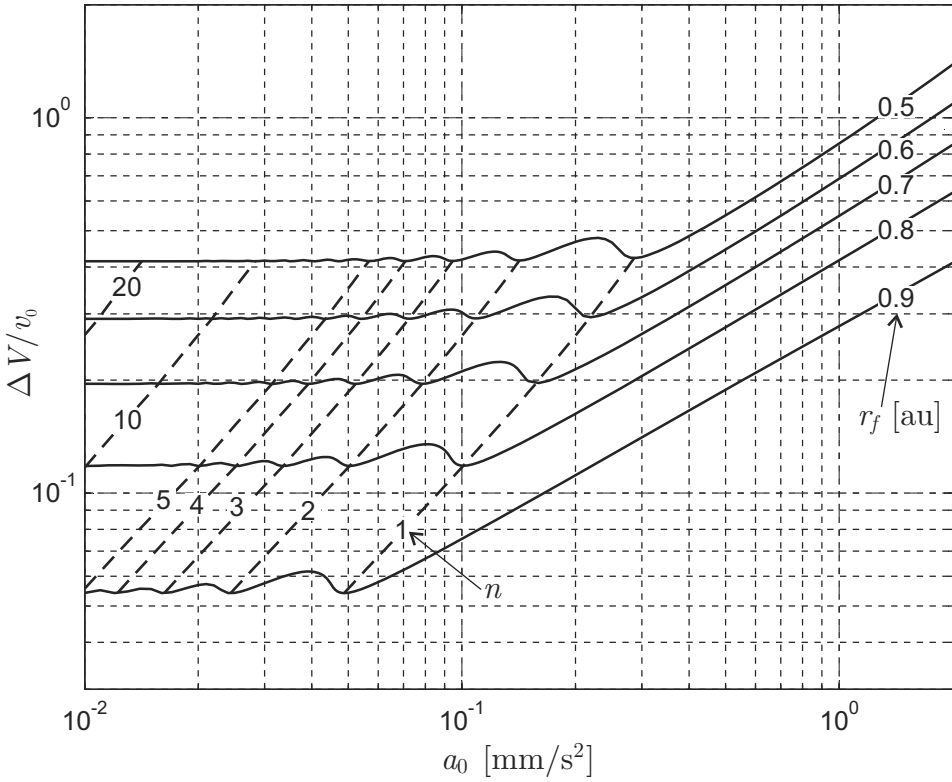


(b) Inner transfer ($r_f < r_0$).

Figure 3. Transfer performance as a function of a_0 and r_f with $I_{sp} = 3000$ s.

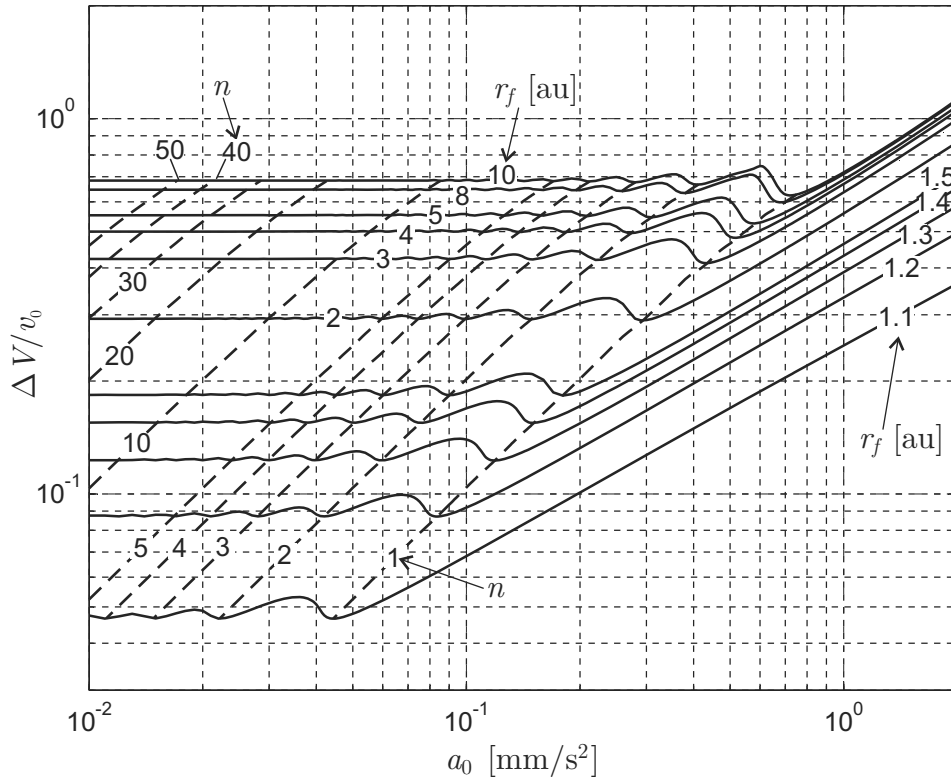


(a) Outer transfer ($r_f > r_0$).

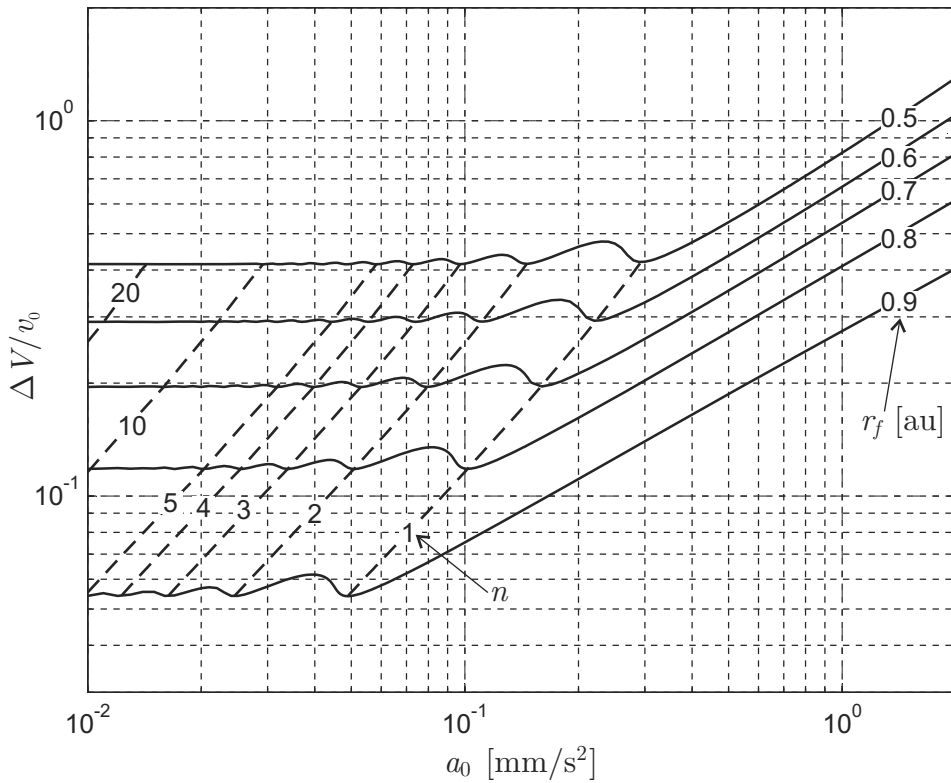


(b) Inner transfer ($r_f < r_0$).

Figure 4. Transfer performance as a function of a_0 and r_f with $I_{sp} = 4000$ s.

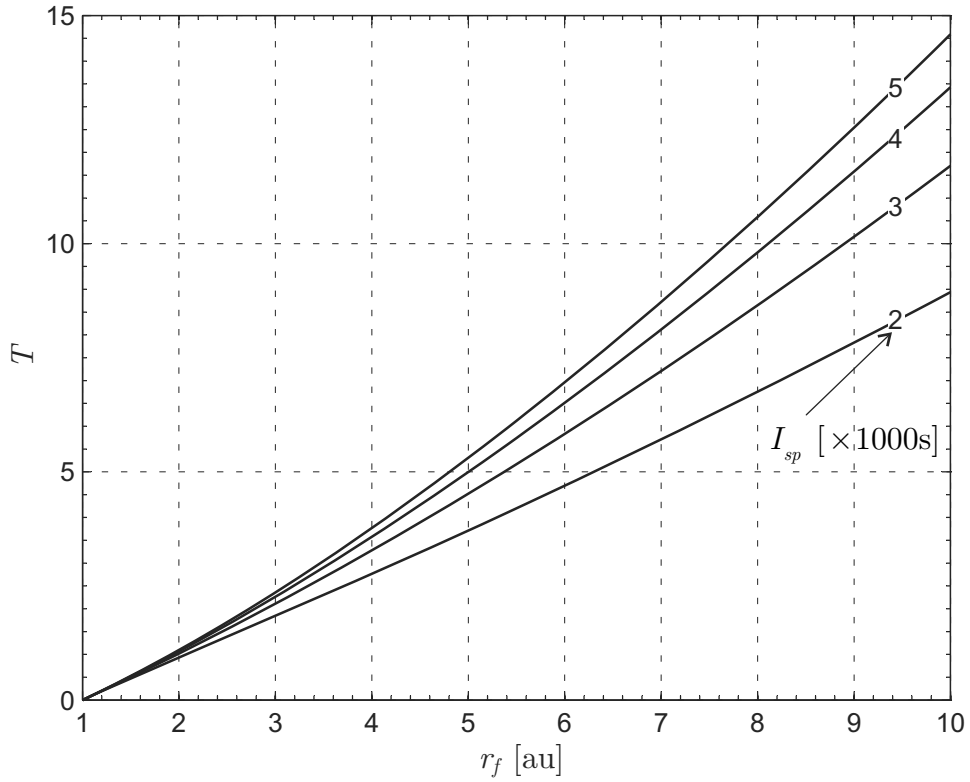


(a) Outer transfer ($r_f > r_0$).

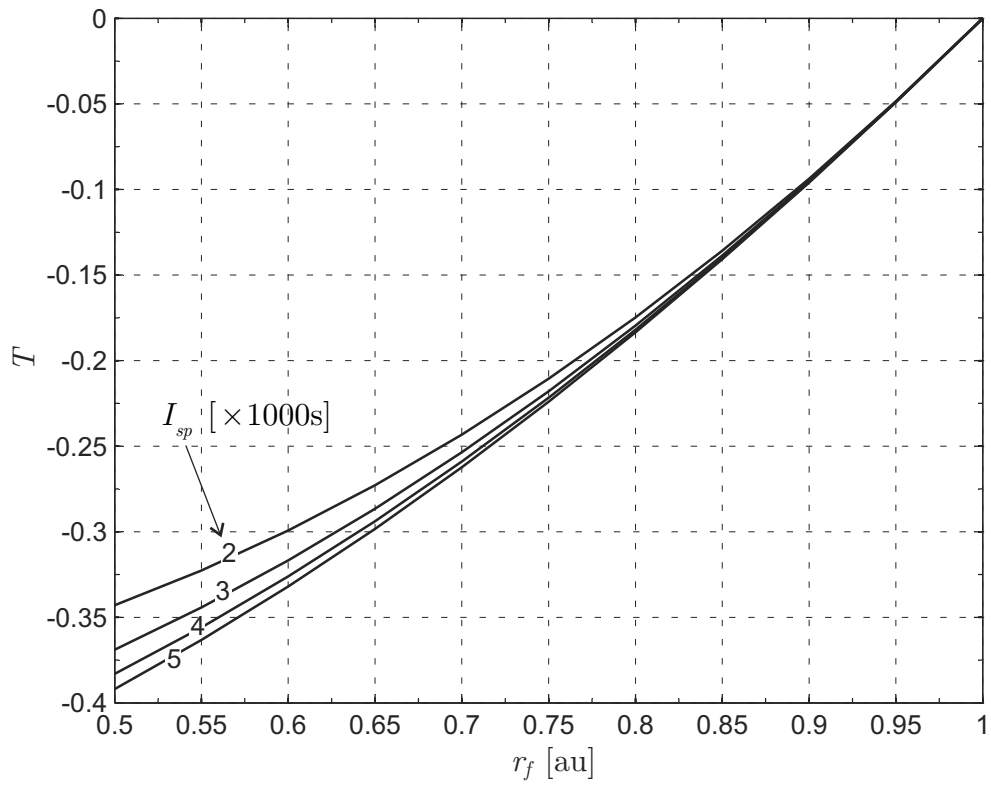


(b) Inner transfer ($r_f < r_0$).

Figure 5. Transfer performance as a function of a_0 and r_f with $I_{sp} = 5000$ s.

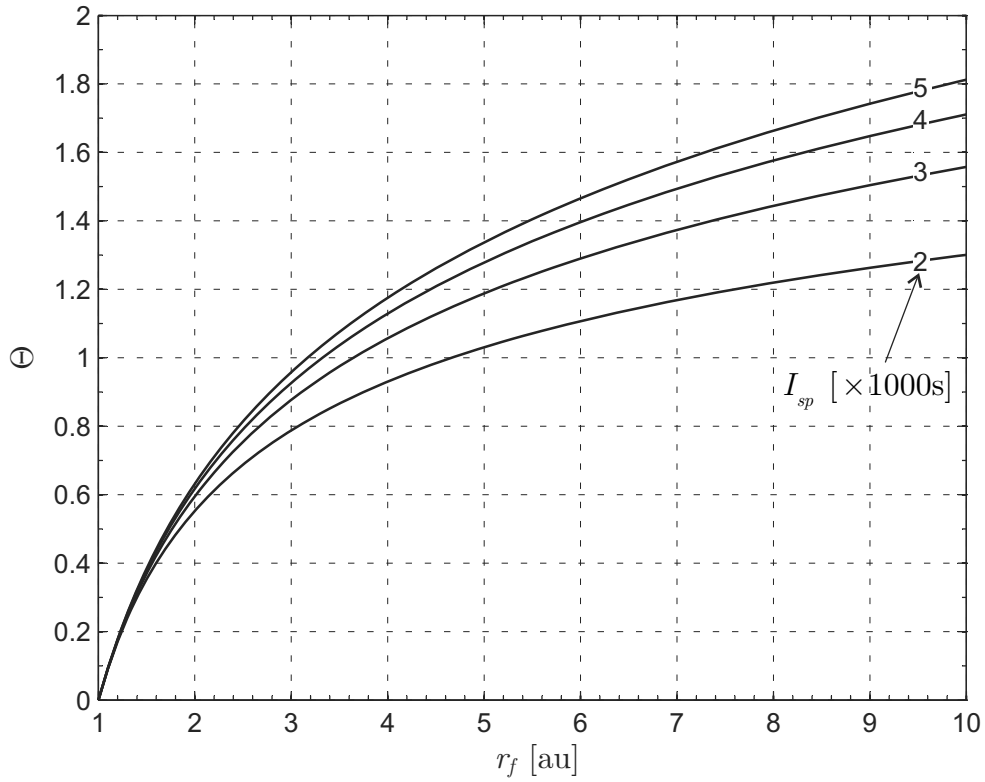


(a) Outer transfer ($r_f > r_0$).

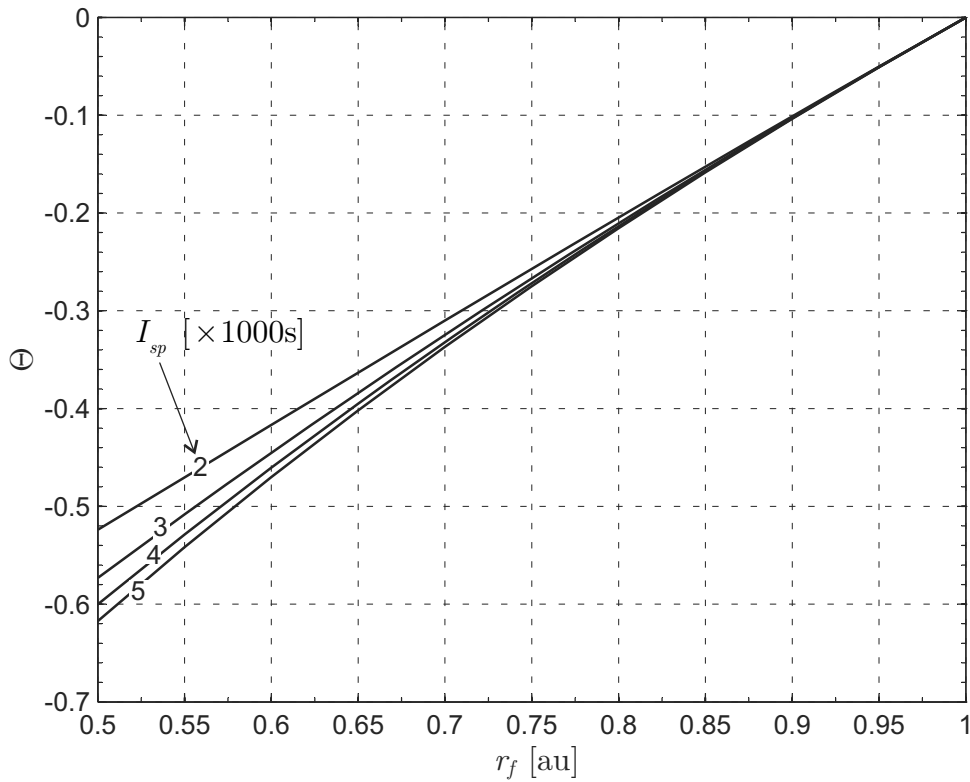


(b) Inner transfer ($r_f < r_0$).

Figure 6. Dimensionless time parameter T as a function of r_f and I_{sp} , see Eq. (32).

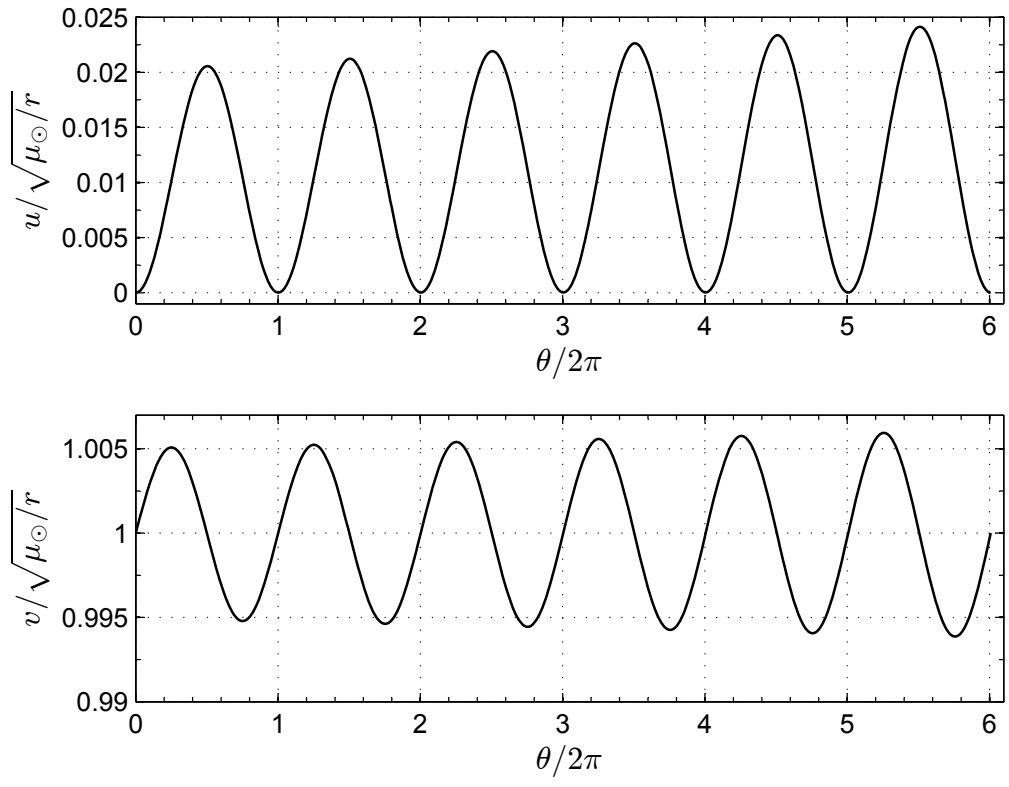


(a) Outer transfer ($r_f > r_0$).

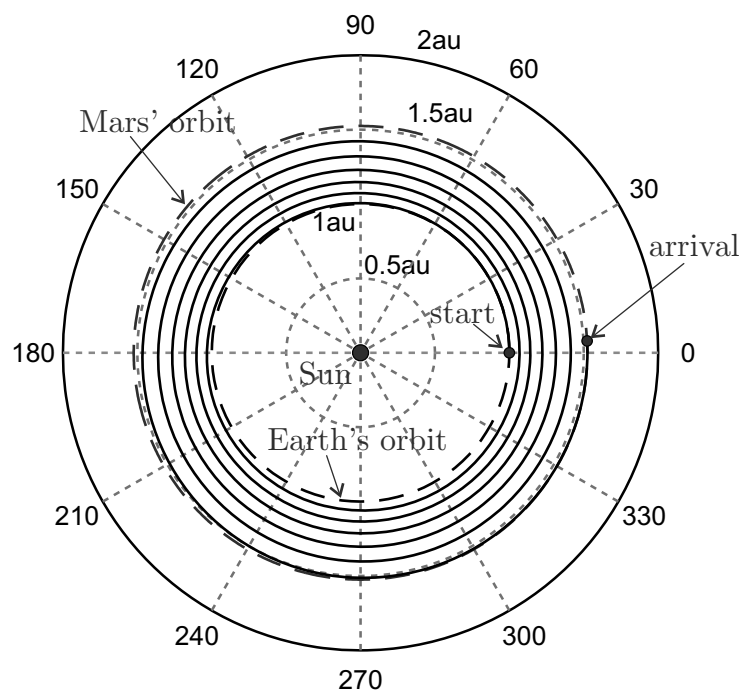


(b) Inner transfer ($r_f < r_0$).

Figure 7. Dimensionless angle parameter Θ as a function of r_f and I_{sp} , see Eq. (34).



(a) Components of the spacecraft's velocity.



(b) Optimal transfer trajectory.

Figure 8. Earth-Mars optimal circle-to-circle transfer when $a_0 = 0.03 \text{ mm/s}^2$, $I_{sp} = 3000 \text{ s}$.

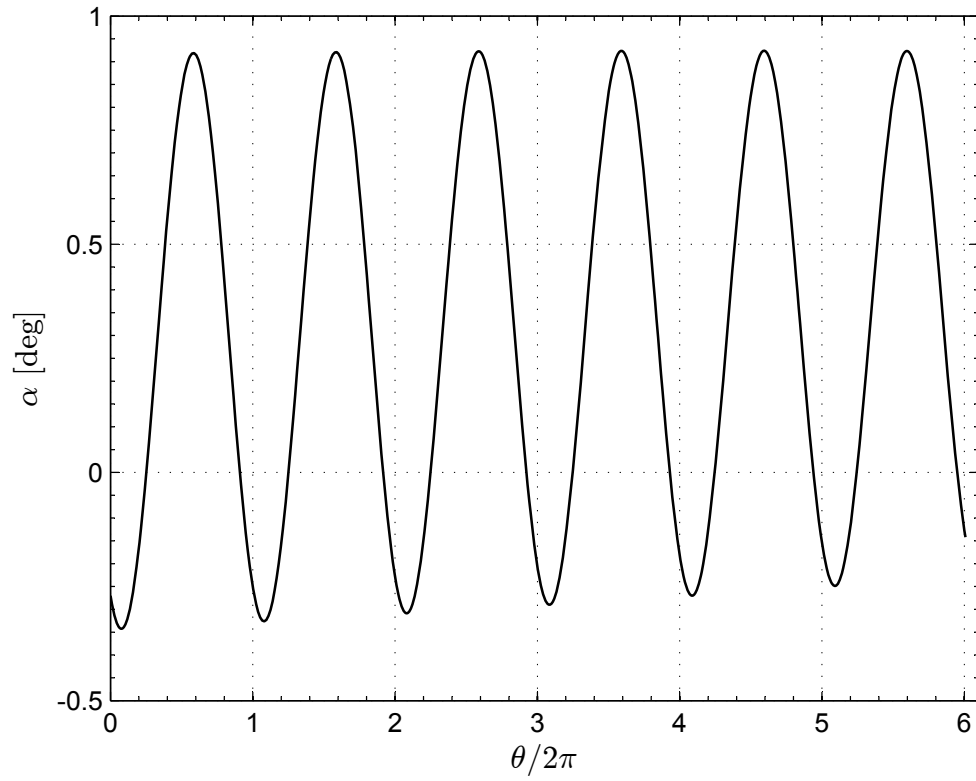


Figure 9. Thrust angle time history (Earth-Mars transfer, $a_0 = 0.03 \text{ mm/s}^2$, $I_{sp} = 3000 \text{ s}$).